Supporting Information

Robichaux et al. 10.1073/pnas.1324215111

SI Methods

Generation of BAC-Tg-ephrinB1-rtTA Mice. *BAC-Tg-ephrinB1-rtTA* (abb: *ephrinB1-rtTA*) mice contain the second-generation reverse tetracycline transactivator, *rtTA-2sM2*, knocked into the ORF of BAC *ephrinB1* sequences. Transgenic mice were generated as follows: BAC clone RP23-110A15, a BAC from a C57BL/6J background containing 27 kb upstream of the ephrin-B1 start codon, was purchased from the BACPAC resources center at the Children's Hospital Oakland (Oakland, CA). The cDNA for *rtTA-2sM2* was targeted into the *ephrin-B1* ORF in RP23-110A15 using bacterial homologous recombination (http://web.ncifcrf.gov/research/brb/recombineeringInformation.aspx). Briefly, RP23-110A15 was first transformed into EL250 strain cells, and then targeted with a modified pL451 vector containing an Frt-sandwiched Neo/Kan cassette and the cDNA for *rtTA-2sM2*, flanked by 500-bp homology arms (the targeting vector is thus *500bpLHA-rtTA-2sM2-Frt/Neo/Kan/Frt-500bpRHA*) guiding the cassette to the ORF of *ephrinB1*. Arabinose induction of *flpe* activity in the targeted BAC was then used to excise the Frt-Neo/Kan-Frt cassette, leaving *rtTA-2s-M2* followed by a single copy of *Frt* in the ephrinB1 ORF. Proper targeting of the *ephrinB1* ORF was confirmed by PCR and restriction endonuclease digests. Pronuclear injection of fertilized oocytes with this *BAC-Tg-ephrin-B1-rtTA* construct was performed by Transgenic Core facilities at the Department of Developmental Biology, The University of Texas Southwestern Medical Center. $EphrinB1^{rtTA}$ mutants were cross bred with *TetO-tdTomato* mice to yield the $ephrinB1^{rtTA}$;*TetO-tdTomato* reporter line. Doxycylcine (Dox) induction of *ephrinB1-rtTA*;*TetO-tdTomato* animals was performed systemically for ∼48 h by feeding animals Dox-treated chow (0.625 g/kg Dox hyclate, Harlan TD.08541) and including Dox in the drinking water (3 mg/mL).

Analysis of Axon Guidance Errors. L1-CAM– or GFP-immunolabeled brain sections, dye-labeled sections, and counterstained sections were imaged on an epifluorescent microscope. Photomicrograph images were produced using an Olympus DP70 CCD digital camera. Confocal *z*-stack images were obtained on a Zeiss LSM 510 Meta confocal microscope and *X-Y-Z* plane image analysis was performed with Volocity software (Perkin-Elmer). Pseudocoloring and adjustments in image brightness, contrast, and color balance were made for image clarity. Ventral telencephalon (VTel) axon guidance misprojection errors were scored, under experimenter-blinded conditions, as L1-CAM^{+} fibers that turned in a ventral fashion away from the internal capsule. The moderate misprojection phenotype was classified by the observation of a few thin axon bundles that became misprojected, whereas severe misprojection brains were classified by the presence of several misprojected fibers or thick misprojected fiber bundles.

1-NA-PP1 Administration. 1-NA-PP1 was synthesized as described previously (1, 2), and timed-pregnant wild-type (WT) or *AS-EphB* dam were injected s.c. twice daily with 80 mg/kg 1-NA-PP1 (dissolved in 10% DMSO, 20% Cremaphor-EL, 70% saline) before L1-CAM analysis at E19 (2).

Data Analysis. The Chi square analysis and Fisher's exact test were used to determine statistical significance in the axon misguidance phenotype scoring experiments. Statistics were compiled and graphs were designed using GraphPad Prism software.

1. Blethrow J, Zhang C, Shokat KM, Weiss EL (2004) Design and use of analog-sensitive protein kinases. *Curr Protoc Mol Biol* 66:18.11.1–18.11.19.

2. Soskis MJ, et al. (2012) A chemical genetic approach reveals distinct EphB signaling mechanisms during brain development. *Nat Neurosci* 15(12):1645–1654.

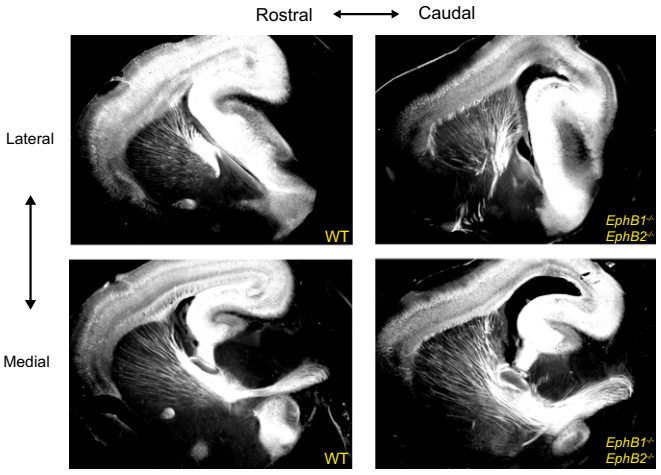

Fig. S1. Axon misprojections in EphB-deficient mice are localized in the lateral VTel. Sagittal vibratome sections of either P0 WT or $EphB1^{-/-}EphB2^{-/-}$ *DKO* mutant brains at a matching medial and lateral sagittal plane. Misprojected axons are largely present in the lateral *DKO* aspect. In addition, the rostral–caudal topography of axons in the VTel is maintained in *DKO* mutants.

A

	# brains with **no** misprojections	# brains with **any** misprojections	n-value
WT	13	1	14
EphB1$^{-/-}$	1	13	14
EphB1$^{Tr/Tr}$	0	9	9
EphB2$^{-/-}$	12	0	12
EphB2$^{Tr/Tr}$	7	0	7
EphB1$^{-/-}$EphB2$^{-/-}$	0	11	11
EphB1$^{Tr/Tr}$EphB2$^{Tr/Tr}$	1	5	6
AS-EphB Vehicle	5	0	5
AS-EphB Drug	1	10	11

**** p<0.0001 (Chi Square test)

B

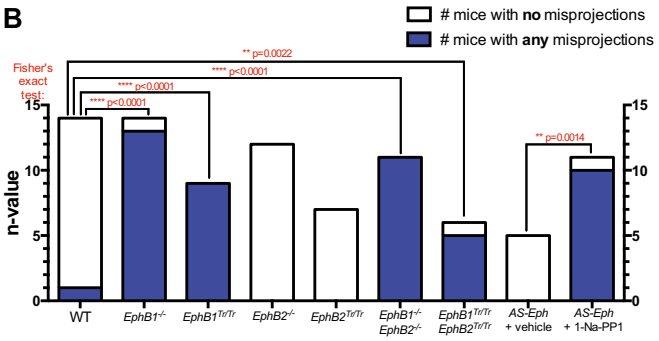

Fig. S2. EphB mutants have a statistically significant axon misprojection phenotype. (*A*) Contingency table of scored axon misprojection phenotypes outlined in Fig. 2*G* for Chi square statistical analysis. All mutant misprojection scores from Fig. 2*G* are combined in the second column. (*B*) Graphical representation of *A* with *P* values from Fisher's exact tests performed to directly compare various mutant genotypes.

A

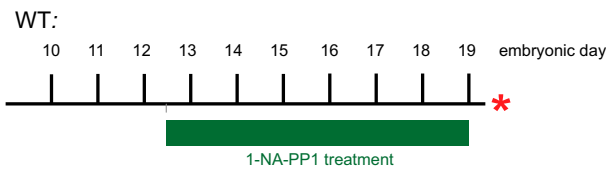

B

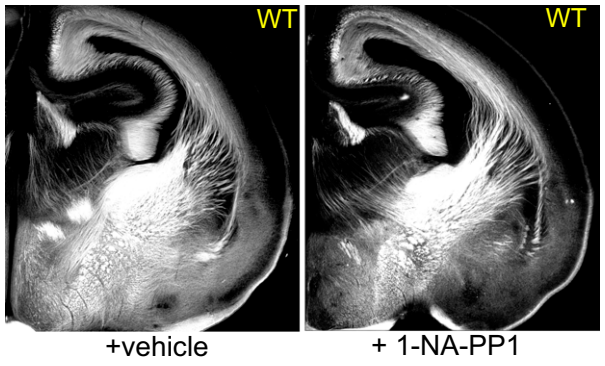

Fig. S3. WT embryos have normal VTel axon morphology upon 1-NA-PP1 drug adminstration. (*A*) Drug injection schedule for 1-NA-PP1 drug treatment of timed-pregnant WT mutants. These mice were administered twice-daily s.c. injections of 80 mg per kg of body weight 1-NA-PP1 or vehicle from E12.5 to E19.0. Embryos were collected for analysis at E19.5 (asterisk). (*B*) Representative L1-CAM–stained E19.5 coronal sections of WT embryos that were either administered 1-NA-PP1 or vehicle and immunostained with anti–L1-CAM. For both conditions, WT embryonic brains have normal L1-CAM^{+} VTel axon morphology (drug, $n = 6$; vehicle, $n = 4$).

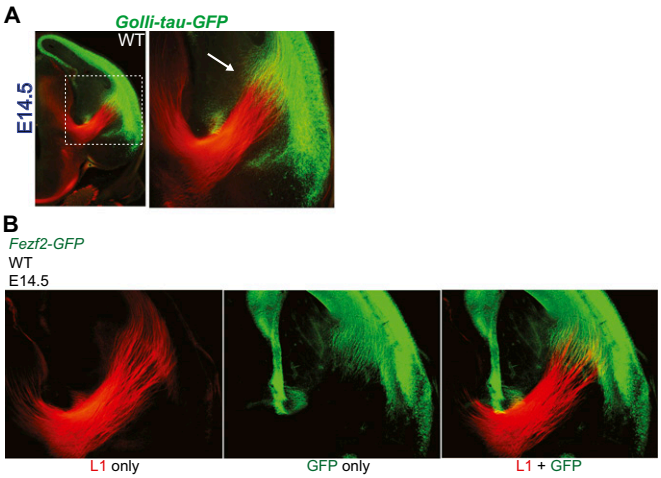

Fig. S4. L1-CAM$^+$ axons in the VTel are clearly derived from the thalamus at age E14.5. (*A*) E14.5 coronal brain section of a *Golli-tau-GFP* reporter embryonic mouse that is also WT for EphB expression, and which demonstrates the partial development of GFP$^+$ cortical pioneer axons in the early VTel (white arrow in *Inset*). (*B*) Coronal section of an E14.5 *Fezf2-GFP* embryonic brain that has WT EphB receptor expression and is immunostained with anti–L1-CAM (red), anti-GFP (green) and dual stain merged. L1-CAM$^+$ axons are clearly derived from the thalamus and ascend toward the cortical intermediate zone (IZ). GFP$^+$ cortical pioneer axons have only penetrated the dorsal half of the developing VTel at this early embryonic age (arrow in *A*), whereas L1-CAM$^+$ thalamocortical axons (TCAs) have developed extensively through the VTel toward the cortical IZ.

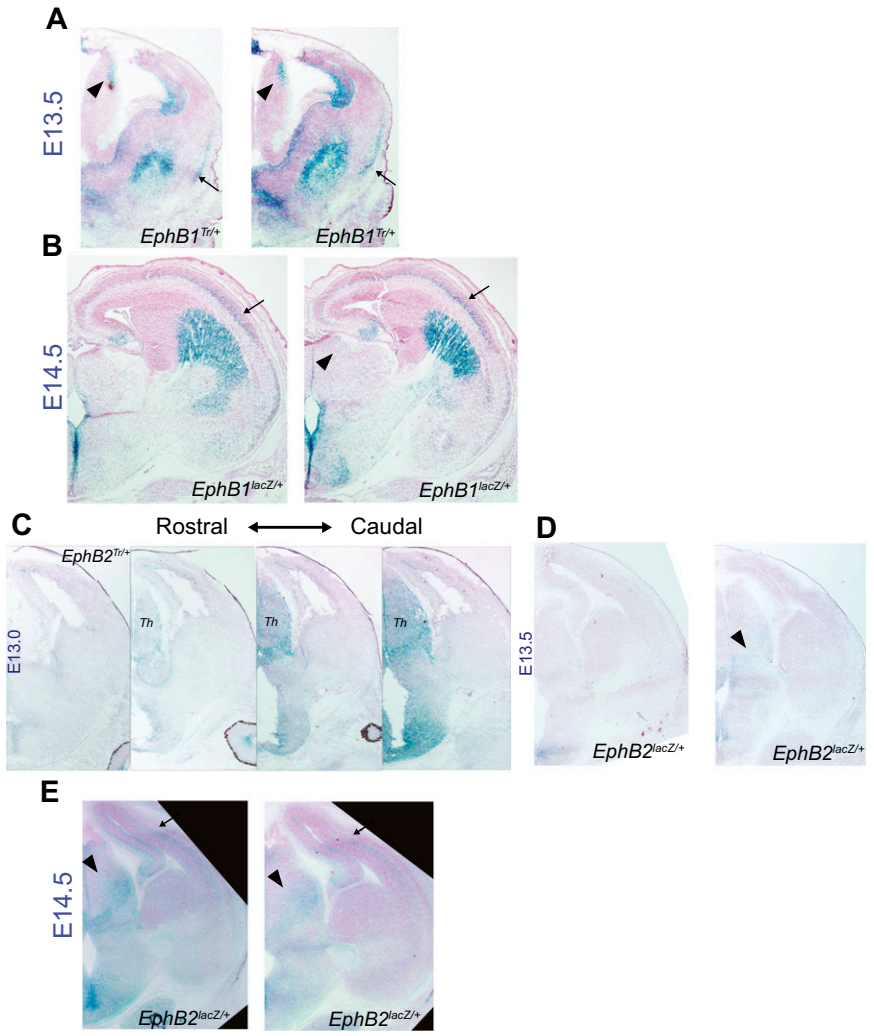

Fig. S5. EphB1 and EphB2 are not expressed in the cortical plate until age E14.5. Coronal brain sections of *EphB1*$^{Tr/+}$ truncated mutants at embryonic age (*A*) E13.5 and (*B*) E14.5 that are stained with X-gal to label β-galactosidase containing EphB1 truncated receptor protein. EphB1 protein expression is concentrated in the dorsal–caudal thalamus (Th) (arrowheads) and cortical plate (arrows). At E13.5, cortical EphB1 expression is exclusive the lateral cortical plate. (*C*) An E13.0 *EphB2*$^{Tr/+}$ mutant brain stained with X-gal. EphB2 expression is ubiquitously expressed throughout the caudal thalamus ($n = 3$). (*D*) E13.5 and (*E*) E14.5 *EphB2*$^{Tr/+}$(also annotated as *EphB2*$^{lacZ/+}$) mutant brains stained with X-gal. EphB2 expression continues throughout the caudal thalamus (arrowheads), and becomes expressed in the cortical plate at E14.5 (arrows).

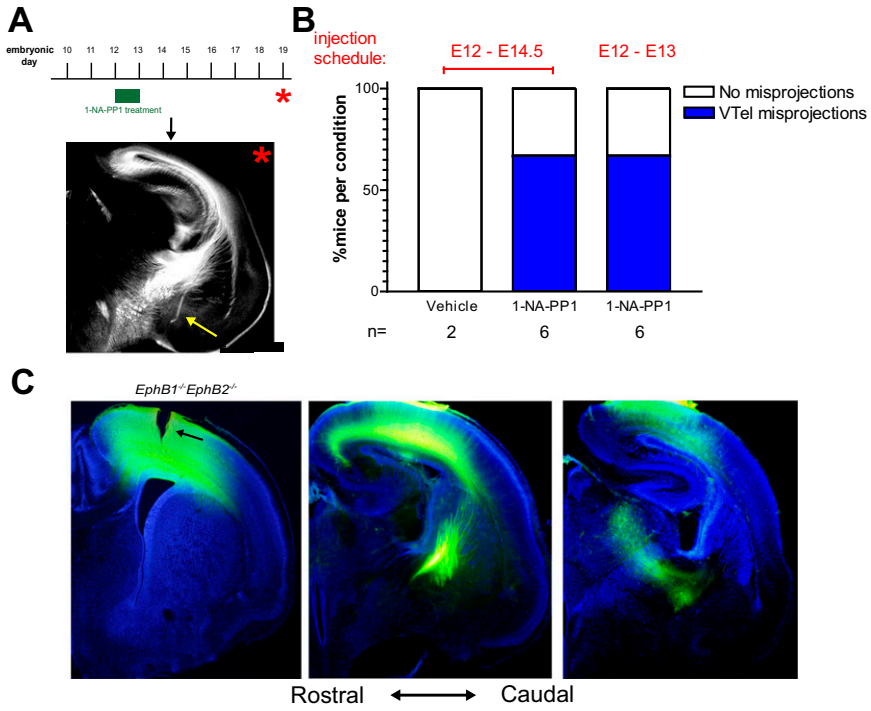

Fig. S6. Anterograde dye tracing from the neocortex labels the entire length of descending cortical axons. (*A*) Drug injection schedule for short-term 1-NA-PP1 drug treatment in timed-pregnant *AS-EphB* mutants. Twice-daily injections of 80 mg per kg of body weight drug were administered for the embryonic time points indicated (green box). Embryos were collected for analysis at E19.0 (asterisk) and fixed for immunoanalysis with anti–L1-CAM. Short-term injected (E12–13) *AS-EphB* mutant dams produced L1-CAM^{+} VTel axon guidance errors (yellow arrow) when analyzed at E19 (graph). (*B*) Graphical representation of VTel misprojections observed from short-term vehicle and 1-NA-PP1 exposure experiments outlined in Fig. 6*B*. (*C*) P0 coronal sections of an *EphB1/2 DKO* brain at postnatal day P0 that are labeled with NV-Jade tracer that is implanted into the dorsal neocortex (black arrow). Descending corticofugal axons from this neocortical origin point are labeled along their entire shaft length through the VTel, IC, and Th. Labeled axons from this example *DKO* brain do not become misprojected in VTel. Brain sections were counterstained with Hoechst nuclear stain (blue).

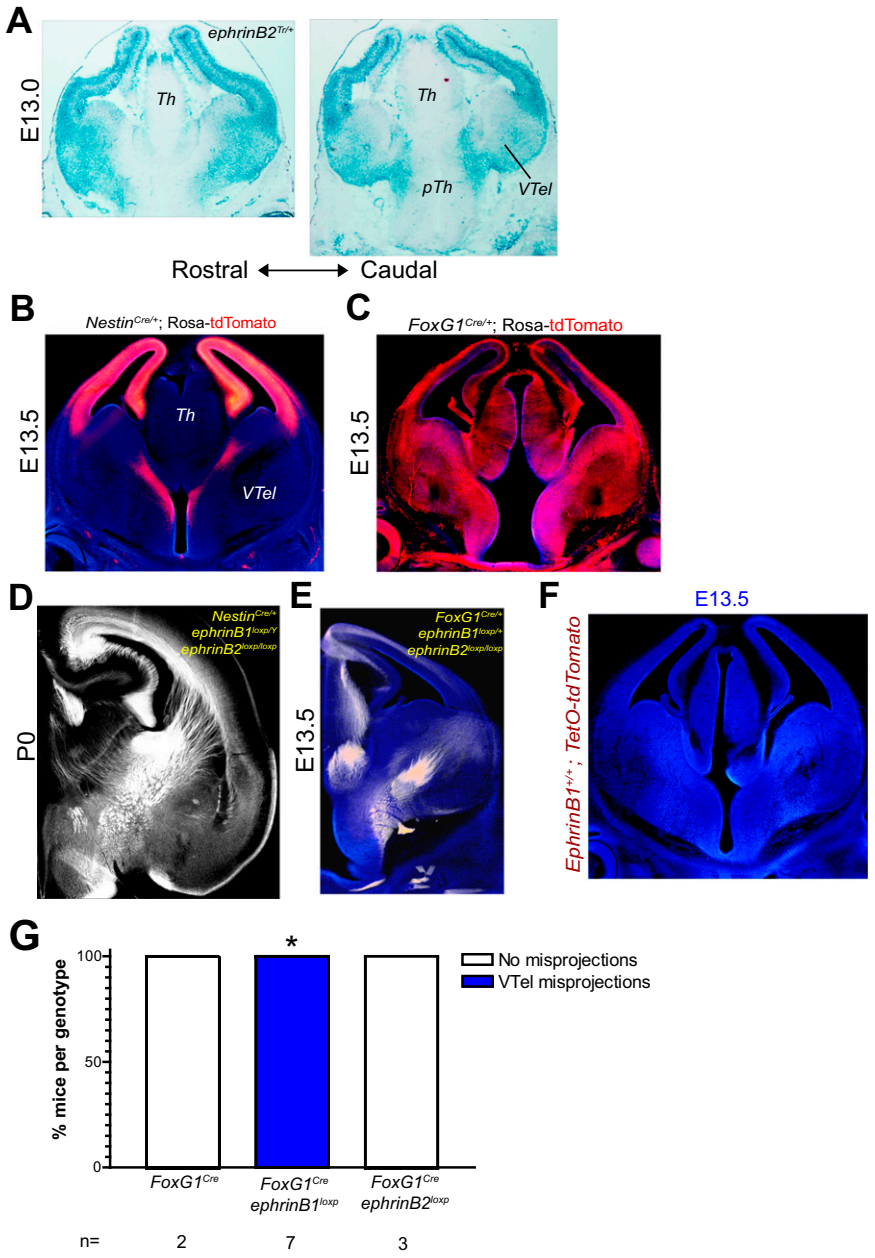

Fig. S7. EphrinB2 is not required for proper TCA guidance in the VTel. (*A*) Coronal brain sections of an *ephrinB2*$^{Tr/+}$ truncated mutant brain at embryonic age E13.0 stained with X-gal to label β-galactosidase containing ephrinB2 truncated receptor protein. At this age, ephrinB2 is highly expressed throughout the entire telencephalon including in the VTel where TCA axons are located; however, ephrinB2 is only lightly expressed in the thalamus (Th) and prethalamus (pTh) ($n = 3$). (*B*) Representative coronal section of an E13.5 embryonic brain containing the Nestin-Cre driver allele and *Rosa-tdTomato* reporter gene. Tomato signal (red) represents Nestin-Cre expression, which is specifically localized to the dorsal telencephalon including the developing cortical plate and hippocampal anlage, as well as migrating cells at the ventral midline. (*C*) Coronal section of a P0 *ephrinB1*$^{loxp/Y}$;*ephrinB2*$^{loxp/loxp}$ conditional mutant containing the Nestin-Cre driver allele. These conditional knockout (cKO) brains have normal axon wiring ($n = 6$), which indicates that the Nestin-Cre driven conditional deletion of ephrinB1/2 is not sufficient to phenocopy EphB receptor KO axon miswiring phenotypes. (*D*) Representative coronal section of an E13.5 embryonic brain containing the FoxG1-Cre driver allele and *Rosa-tdTomato* reporter gene. Unlike Nestin-Cre, FoxG1-Cre expression (red) at this age is ubiquitously expressed throughout the entire brain and other regions of the embryonic head ($n = 3$). (*E*) Coronal brain section of an E13.0 *ephrinB1*$^{lox/+}$;*ephrinB2*$^{loxp/loxp}$ cKO embryo containing the FoxG1-Cre driver allele. These cKO embryos also have normal TCA axon wiring at this early age ($n = 3$) demonstrating that a single copy of ephrinB1 is sufficient for proper TCA axon development, and that ephrinB2 in VTel is not necessary for the proper guidance of these axons. (*F*) Control brain section of an *ephrinB1*$^{+/+}$;*TetO-tdTomato* reporter embryo at age E13.5 that is clear of nonspecific tdTomato fluorescence. (*G*) Combined graphical representation of VTel misprojection scores from FoxG1-Cre driven ephrinB1 (both male *ephrinB1*$^{loxp/Y}$ hemizygous and *ephrinB1*$^{loxp/loxp}$ homozygous females) and ephrinB2 cKO mutants at E13.0 outlined in Fig. 7 *B* and *C*, respectively, compared with *FoxG1*$^{Cre/+}$ controls. *$P < 0.05$, Fisher's exact test.

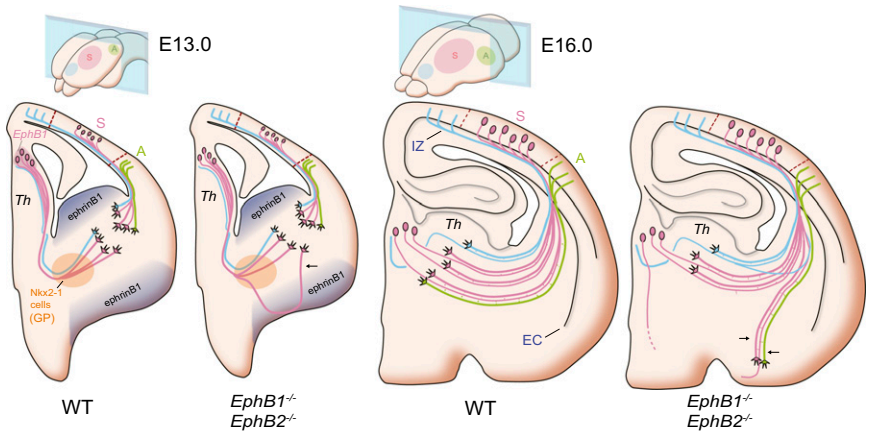

Fig. S8. Model of EphB1-dependent cortical and thalamic wiring in the VTel. Diagrams of cortical-thalamic wiring at embryonic age E16.0 in WT and *EphB1/2 DKO* conditions. A subpopulation of descending cortical fibers from the putative somatosensory cortex (pink S) and auditory cortex (green A) selectively cofasciculates along TCA misprojections that originate, in part, from the caudal thalamus where EphB1 is highly expressed.

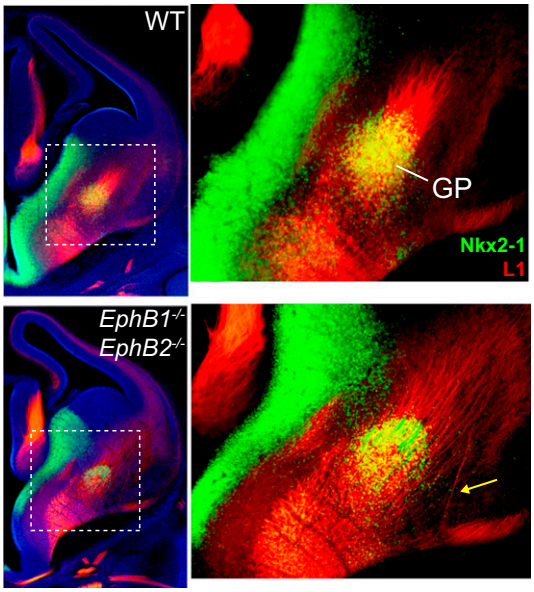

Fig. S9. TCA axons traverse the Nkx2.1 corridor in the VTel. E14.5 coronal brain section of a WT and *EphB1*$^{-/-}$*EphB2*$^{-/-}$ knockout mice that are dual-immunostained with anti–Nkx2-1 (green) and anti–L1-CAM (red). Nkx2-1–labeled cells (green) are localized in the GP regions of the VTel, and L1-CAM^{+} TCA fibers pass directly through this cell population (WT, $n = 2$; *EphB1/2 DKO*, $n = 4$). The L1-CAM^{+} misprojection in the *EphB1/2 DKO* mutant brain (arrow) is located lateral to the Nkx2-1–positive GP region.